Cosmic ray decreases affect atmospheric aerosols and clouds: Auxiliary material

Henrik Svensmark,[1] Torsten Bondo,[1] and Jacob Svensmark[1]

1. Variations in the Primary Cosmic Ray Spectrum Caused by FD

To determine the change in ionization in the atmosphere during a Forbush decrease (FD) variations of the primary cosmic ray spectrum at the top of the Earths atmosphere must be determined. Therefore cosmic ray responses in neutron monitors (NM) and in muon telescopes are studied. Different detectors give information to different parts of the cosmic ray energy spectrum, which will be used to estimate the variation of the primary spectrum. The analysis combines data from the global network of 130 NM (1) and from the Multi-Directional Cosmic-Ray Muon Telescope at Nagoya(2).

NM count mainly the neutrons that are produced in the secondary shower events following the nuclear interactions of the primary cosmic ray particles with the atoms high in the Earth's atmosphere. Count rates and their variations during a FD depend on the altitude and geomagnetic position of the instrument. The counts that a NM registers can be expressed as

$$N(t) = \int_{P_c}^{\infty} S(h,P)J(P,t)dP, \tag{1}$$

where P_c is the cutoff rigidity due to the geomagnetic field,$S(h,P)$ is the yield function (the average number of counts in the NM due to a primary cosmic ray particle of rigidity P), h is the height of the NM above sea level, and $J(P,t)$ is the differential rigidity spectrum at 1 AU as a function of time t.

From the above equation one can define P_m, the median rigidity as

$$N(t)/2 = \int_{P_c}^{P_m} S(h,P)J(P,t)dP, \tag{2}$$

i.e. the rigidity below which the NM registers half its counts. The median rigidity characterizes a NM, since it depends on the location. One problem with this measure is that it changes through the solar cycle. However, this is not a serious matter in the present study, since the FD with which we are dealing are most frequent around solar maximum. We elect to use the median rigidity at solar maximum for all NM. The median rigidity of the NM data is based on vertical cut-off rigidity estimates and ranges from ≈10 GV (South Pole stations) to ≈47 GV (Ahmedabad, India). The 17 different viewing angles of the Multi-directional Nagoya detector represent 17 different paths of the muons through the atmosphere and therefore 17 different response functions. The median rigidity range of the Muon Telescope ranges from 60 to 119 GV (2). So the present work covers a range from 10 GV to 119 GV in median rigidity, and the results are based on daily averages. Figure S1 shows how the relative changes in counts vary across that range of median rigidities.

The availability of data on clouds from the SSM/I instruments of the Defence Meteorological Satellite Program, since 1987, defines the period 1987-2007 over which FD are studied. (AERONET data on aerosols are available since 1998.) During the period of interest FD are identified as a sudden decrease in the neutron counts followed by a recovery over days to weeks. First the day at which the minimum counts, $N(i_{\min})$, occurs is found. Then a reference level of the neutron counts is found prior to the minimum of the FD defined as

$$N_R = \frac{1}{14}\sum_{i_{min}-15}^{i_{min}-1} N(i), \tag{3}$$

i.e. a 14 day average of the neutron counts ending 1 day before the minimum. From this the change in neutron counts is defined as

$$\Delta N = N_{i_{min}} - N_R, \tag{4}$$

and the relative change is defined as

$$\delta N = \frac{\Delta N}{N_R}. \tag{5}$$

Table S1 shows the 26 largest FD events identified in this way. For comparison see (Kudela 2004) (3).

The 130 NM located all over the world, at different altitudes and with different cutoff rigidities, are used to determine the the above relative change for a particular FD $\delta N_{i,k}$, where the index i identifies the NM, and index k the FD. For each FD the relative change in $\delta N_{i,k}$ is related to the station's median rigidity $(P_m)_i$, and a function

$$n_k = A_k (P_m)^{-\gamma_k}, \tag{6}$$

where A_k and γ_k are determined by minimizing the least square deviation to the data . The form of the above function is regularly used and to a good approximation seen in FD modulations of energy spectra (4).

It is possible to relate the foregoing NM responses to changes in $J(P,t)$, the differential rigidity spectrum at 1 AU, by the relation $P_m \rightarrow P$ such that

$$\frac{\delta J_k}{J_k} \approx A_k P^{-\gamma_k}. \tag{7}$$

Figure S2 shows an exact calculation where the primary spectrum is assumed of the form in Eq. (7). Using a yield function for an NM-64 neutron monitor (5) it is therefore possible, using Eq. (2) and Eq. (7) and Eq. (5), to calculate both P_m and $\delta N/N$ as a function of a station's cutoff

rigidity and altitude. The figure demonstrates for a particular FD that the approximation Eq. (7) is satisfactory to within 10%. The main errors are for the lower rigidities but those energies are not important for the ionization in the lower troposphere.

In some studies the force field approximation (6) is used to calculate the heliospheric modulation of cosmic rays (7). But this equation does not describe shocks and diffusive fronts in the heliosphere which characterize coronal mass ejections. Therefore the approach involving the median rigidity is preferred.

2. Variation in the Atmospheric Ionization

With the variation in the differential rigidity spectrum known via Eq. (7) it is possible to calculate the resulting change in the ionization down through the atmosphere. This is done by a Monte Carlo simulation of incoming CR energies and the resulting shower structure of secondary particles. The evolution of the shower is calculated by the CORSIKA program (8) where a primary proton of kinetic energy T and an incident angle to zenith $0 \leq \alpha \leq 70$ deg. are the initial conditions for the cascade. For each particle energy in the range 1 - 1000 GeV, 10,000 showers are calculated, and $I(P,h)$, the average ionization energy deposited at various heights in the atmosphere, is obtained. It is then possible to derive the ion production in the atmosphere as

$$q(h) = \int_{P_c}^{\infty} I(P,h) J(P) dP, \tag{8}$$

where $I(P,h)$ is the ionization at height h caused by a particle with rigidity P. The change in ionization due to a FD is then given by

$$\delta q(h) = \int_{P_c}^{\infty} I(P,h) A_k P^{-\gamma_k} J(P) dP. \tag{9}$$

Figures S3a and S3b show the ionization production as a function of the altitude (9). The differential energy spectrum used in the calculations is based on the Bess spectrometer observations of cosmic rays close to solar minimum (10). The black curve (Figure S3a) is the solar minimum curve and the red curve is for the solar maximum, based on A_{SC} and γ_{SC} in the caption of Table S1. The blue curves are the reduction in ion production due to the FD and based on the the A and γ in Table S1. The lowest curve is the exceptional event in October 2003. Figure S3b contains the same information but now the reduction in ion production is normalized with the reduction from solar max to solar min, i.e. the difference between the black curve and the red curve.

3. Examples of Individual Events

The paper makes use of data on aerosols and clouds averaged for 5 FD events. Doing so averages out some of the meteorological noise, so that the impact of GCR reductions is plainer to see. On the other hand, it might be objected that the choice of events is untypical, or that a single FD showing an accidentally large effect dominates the average. We have examined many plots for individual events, and for all of the strongest ones (judged by the change in low-altitude ionization) the features shown in averaged data are repeated. To illustrate this, we show in Figure S4 the loss of cloud liquid water in each of the first six events in Table 1.

References and Notes

1. NM data can be obtained from ftp://cr0.izmiran.rssi.ru/

2. We acknowledge the Cosmic Ray Section, Solar-Terrestrial Environment Laboratory, Nagoya University who provided the muon data. Data can be obtained from http://www.stelab.nagoya-u.ac.jp/ste-www1/div3/muon/muon1.html

3. K. Kudela, *J. Atmos. & Solar Terr. Phys.*, **66**, 1121 (2004).

4. H. S. Ahluwalia and M. Fikani, *J. Geophys. Res.* **112**, 8105 (2007).

5. J. M. Clem and L. I. Dorman, *Space Sci. Rev.*, **93**, 335 (2000).

6. R. A. Caballero-Lopez and H. Moraal, *J. Geophys. Res.*, **109**, A01101 (2004).

7. Usoskin *et al.*, *J. Geophys. Res.*, **110**, A12108 (2005).

8. More information about CORSIKA can be found at http://www-ik.fzk.de/corsika/

9. For general introduction to ionization in the atmosphere see for example: G. A. Bazilevskaya *et. al*, *Space Sci. Rev.*, DOI 10.1007/s11214-008-9339-y.

10. T. Sanuki et al., *Astro. Phys. J.*, **545**, 1135 (2000).

Figure 1. Relative changes of counts by neutron monitors and the Nagoya Muon Telescope are here plotted against the median rigidity of the stations P_m, for a few FD shown in color. The colored curves are the fitted functions of the form of Eq. (7). The black curve is the fit to the change from solar minimum to solar maximum.

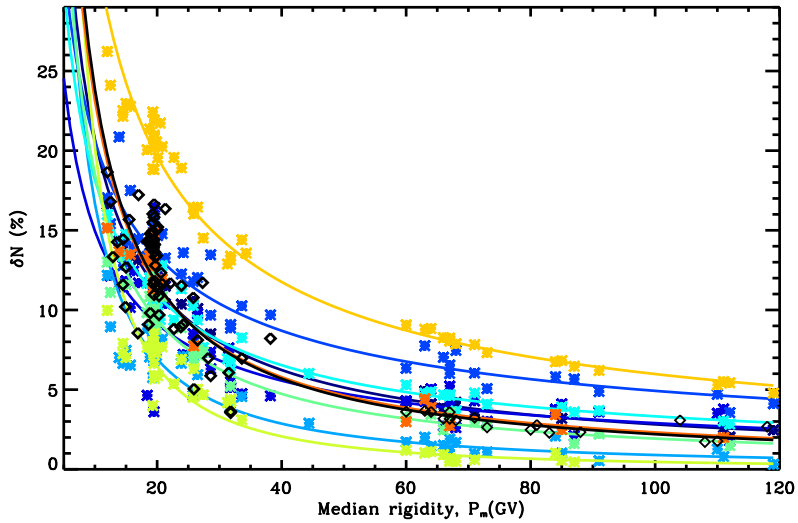

Figure 2. The relative changes in cosmic ray counts diminish as the energies of the primary cosmic ray particles increase. For an explanation of the construction of this plot, see text.

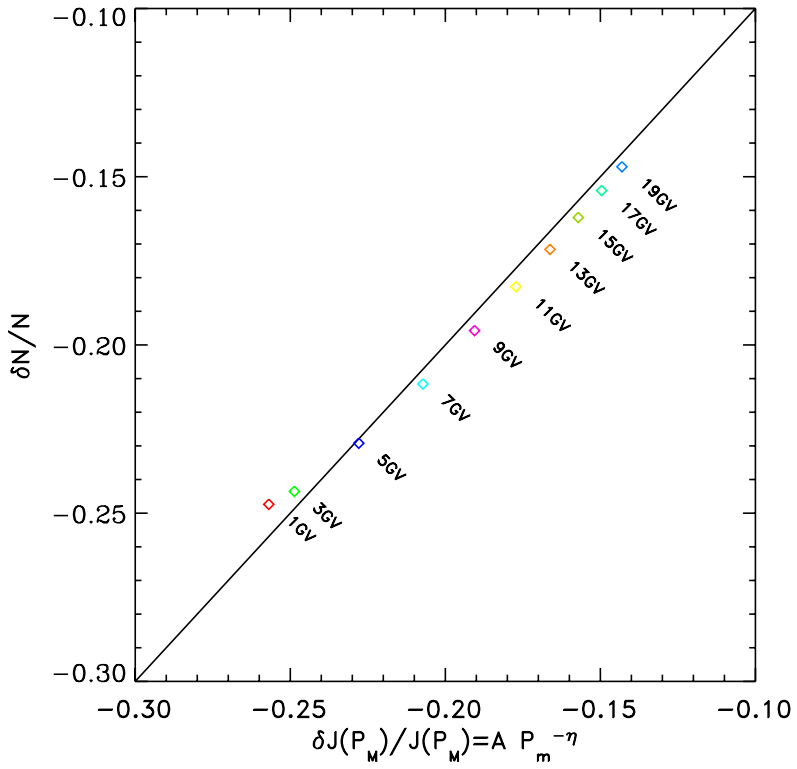

Figure 3. (a) The absolute ion production in the atmosphere (US standard) as a function of altitude. The black curve is the ion production under solar min conditions, and the red curve is during solar max corresponding to a 45 deg. latitude and a cutoff rigidity of 6 GV. The individual blue lines show the depression relative to the solar min conditions due to the FD events in Table S1. The lowermost line is for the very strong FD event in October 2003. (b) The individual FD normalized to the solar cycle variation (the difference between the black curve and the red curve in Figure S3a). Of special interest in the paper are the changes in the lowermost 3 km. Dates are given for the six strongest events at low altitude.

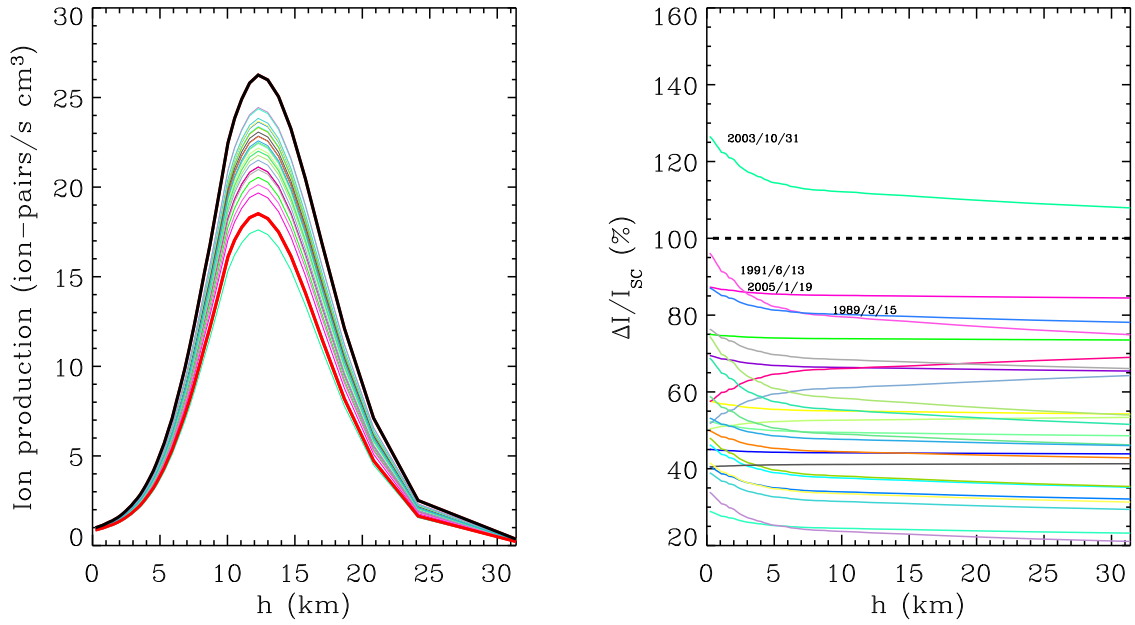

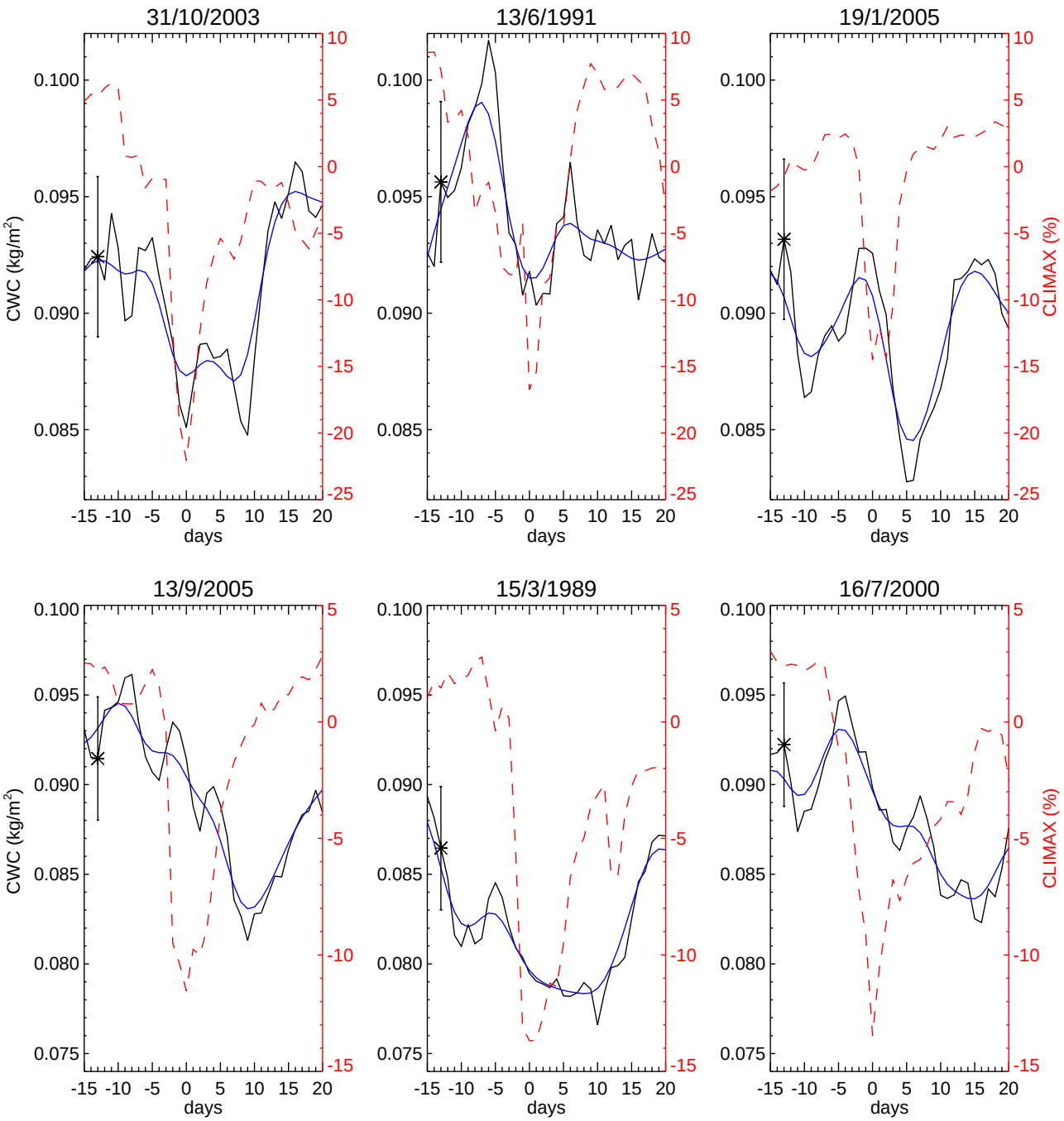
31/10/2003
13/6/1991
19/1/2005
13/9/2005
15/3/1989
16/7/2000
CWC (kg/m^2)
CLIMAX (%)
days

Figure 4. The impact of coronal mass ejections on the liquid water content of clouds is plotted for the six strongest events (order numbers 1-6 in Tables 1 and SM1). The red broken lines show Forbush decreases (FDs) in the influx of galactic cosmic rays (GCRs) as recorded by neutron counts at Climax, Colorado. Each plot covers the period from 15 days before to 20 days after the date of the GCR minimum. The black curves show the daily mean liquid water content of clouds (CWC) over the world's oceans as measured by SSM/I. The blue curves are Gaussian smoothed curves with a width of 2 days and total length of 10 days. The error bar denotes the one sigma natural variability.